

Article

X-ray Structure Analyses and Biological Evaluations of a New Cd(II) Complex with S-Triazine Based Ligand

Kholood A. Dahlous^{1,*}, Atallah A. M. Alotaibi², Necmi Dege³, Ayman El-Faham^{2,*}, Saied M. Soliman^{2,*}
and Heba M. Refaat^{2,*}

¹ Department of Chemistry, College of Science, King Saud University, P.O. Box 2455, Riyadh 11451, Saudi Arabia

² Department of Chemistry, Faculty of Science, Alexandria University, P.O. Box 426, Alexandria 21321, Egypt; atallah1415@gmail.com

³ Department of Physics, Faculty of Arts and Sciences, Ondokuz Mayıs University, Samsun 55139, Turkey; necmid@omu.edu.tr

* Correspondence: kdahlous@ksu.edu.sa (K.A.D.); aymanel_faham@hotmail.com (A.E.-F.); saied1soliman@yahoo.com (S.M.S.); hebarefaat212@yahoo.com (H.M.R.)

Abstract: The crystal structure of a new penta-coordinated Cd(II) complex of the formula [Cd(BPMT)Br₂] was presented. This Cd(II) complex was synthesized by mixing Cd(NO₃)₂·4H₂O and 2,4-bis(3,5-dimethyl-1H-pyrazol-1-yl)-6-methoxy-1,3,5-triazine (BPMT) in the presence of KBr. It crystallized in the monoclinic crystal system and *P*₂/*n* space group. The crystal parameters are *a* = 11.3680(8) Å, *b* = 11.1648(8) Å, *c* = 15.8593(11) Å, and β = 103.563(2)°, while the unit cell volume is 2190.6(12) Å³ and it comprised four molecules. The supramolecular structure of the [Cd(BPMT)Br₂] complex is mainly controlled by the intermolecular Br···H interactions. Hirshfeld calculations predicted the H···H (38.1%), Br···H (24.3%), C···H (11.1%), and N···H (9.5%) interactions are the most dominant. Biological evaluations for the antimicrobial and anticancer properties of the studied complex are presented. The Cd(II) complex has better anticancer and antibacterial activities than the free BPMT ligand. The anticancer activity against lung carcinoma (A-549) is higher for the former (18.64 ± 1.09 µg/mL) compared to the latter (372.79 ± 13.64 µg/mL). Additionally, the best antibacterial activity for the Cd(II) complex was found against *B. subtilis*.

Keywords: X-ray; Hirshfeld; Cd(II); penta-coordinated; anticancer; antibacterial



Citation: Dahlous, K.A.; Alotaibi, A.A.M.; Dege, N.; El-Faham, A.; Soliman, S.M.; Refaat, H.M. X-ray Structure Analyses and Biological Evaluations of a New Cd(II) Complex with S-Triazine Based Ligand. *Crystals* **2022**, *12*, 861. <https://doi.org/10.3390/cryst12060861>

Academic Editor: Marian Valko

Received: 28 May 2022

Accepted: 14 June 2022

Published: 18 June 2022

Publisher's Note: MDPI stays neutral with regard to jurisdictional claims in published maps and institutional affiliations.



Copyright: © 2022 by the authors. Licensee MDPI, Basel, Switzerland. This article is an open access article distributed under the terms and conditions of the Creative Commons Attribution (CC BY) license (<https://creativecommons.org/licenses/by/4.0/>).

1. Introduction

Transition metal complexes have attracted the attention of many researchers due to their versatile applications in biology and for designing drugs that have slow-release and long-action properties [1]. Cadmium (II) complexes have attractive applications in diverse fields, such as electronics and catalysis [2–9]. Free Cd(II) ion has well-known high toxicity on human health, but several studies have revealed that Cd(II) complexes with organic ligands have interesting bio-activities including DNA binding ability [10], antitumor [11], and antibacterial [12] activities. In addition, the organic ligand itself could be employed as a detoxification agent in the case of complexes with high-stability constants [13]. The DNA interactions of Cd(II) via covalent binding interactions between adenine and guanine in DNA were proved by Hossain and Huq [14]. Some Cd(II) complexes have been reported to possess interesting anticancer activity similar to cisplatin [11,15]. From a structural point of view, Cd(II) ion has varied coordination numbers due to its high affinity to form coordinate bonds with a diverse type of ligands, forming a wide range of coordination complexes [16–24].

Pincer ligands are an interesting class of chelating agents which can form stable metal complexes [25,26]. These chelating agents have a diverse number of applications in different fields [27–30]. Among the different categories of these ligands, our research

group is interested with the *s*-triazine pincer ligands due to their powerful chelating efficiency and their simple preparation from cyanuric chloride [31]. *s*-Triazine pincer ligands have a weak ligand field, which supports the synthesis of interesting high-spin complexes for different magnetic applications [32,33]. Additionally, this class of ligands is characterized by the presence of a symmetric triazine core, which is an important feature in crystal engineering [34–44]. On continuation of our interest into the structural aspects and biological applications of *bis*-pyrazolo-*s*-triazine complexes [45–51], the present work aims to synthesize a new Cd(II) complex of the 2,4-*bis*(3,5-dimethyl-1*H*-pyrazol-1-yl)-6-methoxy-1,3,5-triazine (BPMT, Figure 1) ligand, shedding the light on its molecular and supramolecular characteristics. Additionally, its bioactivities as antimicrobial and anticancer agents were assessed.

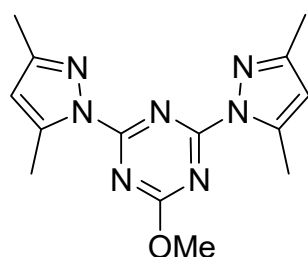


Figure 1. Structure of the BPMT ligand.

2. Materials and Methods

Chemicals, instrumentations, and details of the X-ray single-crystal structure analysis [52–58] are presented in the Supplementary Materials. The synthesis of BPMT is described in Method S1 (Supplementary Materials) [51,52].

2.1. Synthesis of the [Cd(BPMT)Br₂] Complex

The synthesis of the [Cd(BPMT)Br₂] complex was performed by mixing 10 mL ethanolic solution of BPMT (29.9 mg, 0.1 mmol) with Cd(NO₃)₂·4H₂O (30.8 mg, 0.1 mmol) in 5 mL distilled water, followed by the addition of 1 mL of saturated aqueous KBr solution. The resulting solution was left for slow evaporation at room temperature, and colorless crystals of the [Cd(BPMT)Br₂] complex were obtained after 10 days.

Yield; C₁₄H₁₇Br₂CdN₇O; 77%. Anal. Calc. C, 29.42; H, 3.00; N, 17.15; Br, 27.96; Cd, 19.67%. Found: C, 29.20; H, 2.92; N, 17.01; Br, 27.89; Cd, 19.53. IR (KBr, cm⁻¹): 3101, 2991, 1614, 1539.

2.2. Biological Studies

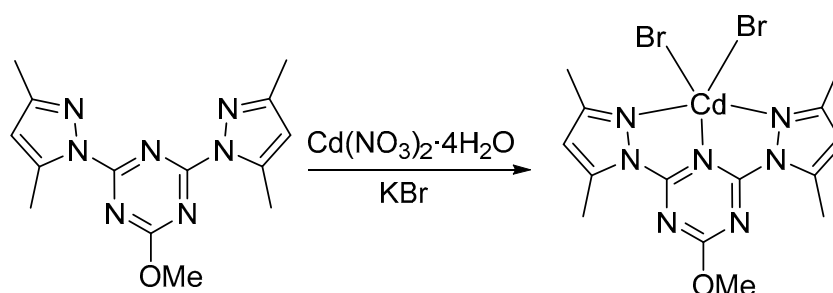
The bioactivities of the studied compounds were determined, and the experimental details are mentioned in Methods S2 and S3 (Supplementary Materials) [59,60].

3. Results and Discussion

3.1. Synthesis and Characterizations

A new Cd(II) complex was self-assembled from the reaction of an aqueous solution of Cd(NO₃)₂·4H₂O with an ethanolic solution of BPMT in the presence of KBr. Owing to the weak coordinating power of the nitrate anion compared to the bromide anion, the corresponding dibromo complex [Cd(BPMT)Br₂] was obtained (Scheme 1). As a soft-metal ion, Cd(II) favored the coordination of the softer Lewis base (Br⁻) rather than the nitrate ion, which acts as an electron-pair donor via the harder oxygen atom. The structure of the Cd(II) complex is confirmed using elemental analysis, FTIR spectra, and the exclusive use of single-crystal X-ray diffraction. Its supramolecular structure was analyzed using Hirshfeld analysis. The FTIR spectra of the [Cd(BPMT)Br₂] complex and the free BPMT ligand are presented in Figures S1 and S2 (Supplementary Materials). The free BPMT ligand showed the aromatic and aliphatic ν_{C-H} modes at 3098 and 2923 cm⁻¹, respectively, while the ν_{C=N} and ν_{C=C} modes were detected at 1615 and 1540 cm⁻¹, respectively. For the

[Cd(BPMT)Br₂] complex, these modes were found slightly shifted to 3101, 2991, 1614, and 1539 cm⁻¹, respectively.



Scheme 1. Synthesis of [Cd(BPMT)Br₂].

3.2. Structure Description of the [Cd(BPMT)Br₂] Complex

The X-ray structure of [Cd(BPMT)Br₂] is shown in Figure 2. This complex is crystallized in the *P*2₁/*n* space group and monoclinic crystal system with crystal parameters *a* = 11.3680(8) Å, *b* = 11.1648(8) Å, *c* = 15.8593(11) Å, and β = 103.563(2)° (Table 1). The unit cell volume is 2190.6(12) Å³ and *Z* = 4. The molecular formula of the [Cd(BPMT)Br₂] complex is C₁₄H₁₇Br₂CdN₇O which represents the asymmetric formula.

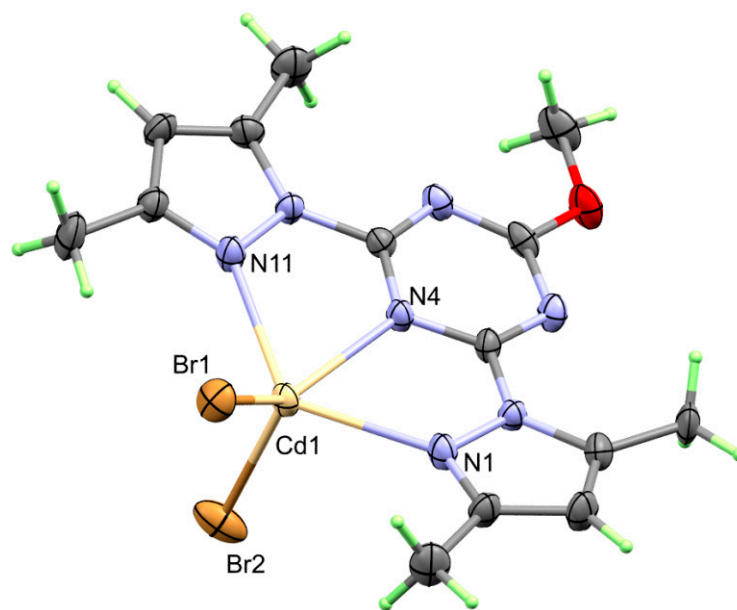


Figure 2. X-ray structure of [Cd(BPMT)Br₂].

In the neutral [Cd(BPMT)Br₂] complex, the Cd(II) is penta-coordinated with a *CdN*₃Br₂ coordination sphere. The **BPMT** ligand acts as a tridentate pincer chelate, with two long and almost equidistant Cd-N bonds with the two pyrazolyl moieties, and one slightly shorter Cd-N bond with the *s*-triazazine core (Table 2). The corresponding Cd-N distances are 2.413(7), 2.417(7), and 2.337(6) for Cd1-N1, Cd1-N11, and Cd1-N4, respectively. The two bite angles, N4-Cd1-N1 and N4-Cd1-N11, of the **BPMT** chelating ligand are the same (66.0(2)°). The values of the bite angles are significantly smaller than the corresponding values for small metal ions (Co(II) [47], Ni(II) [48], and Zn(II) [49]). It is plausible that the large metal ions such as Cd(II) are capable of coordinating with the **BPMT** ligand at longer distances than the small-size metal ions are. As a consequence, the bite angles are found to be smaller in the [Cd(BPMT)Br₂] complex. The results are found to be in good agreement with the structurally related [Cd(BPMT)Cl₂] complex [50]. Additionally, the Cd(II) ion is further coordinated with two bromide ions where the Br1-Cd1-Br2 angle is 115.94(4)°. Of course, the Cd1-Br1 (2.5388(11) Å) and Cd1-Br2 (2.5527(13) Å) bonds are generally longer

than the corresponding values of the dichloro analogue (Cd1-Cl1; 2.406(2) Å and Cd1-Cl2; 2.429(2) Å). On the other hand, the τ_5 parameter that is used for measuring the degree of distortion in the penta-coordinated metal ion is calculated to be 0.112 [61]. Hence, the CdN_3Br_2 coordination geometry is a slightly distorted square pyramidal. The value of the τ_5 parameter is close to that of the structurally related $[Cd(BPMT)Cl_2]$ complex ($\tau_5 = 0.127$).

Table 1. Crystal data and refinement details of $[Cd(BPMT)Br_2]$.

CCDC	2,154,999	
Empirical formula	$C_{14}H_{17}Br_2CdN_7O$	
Formula weight	571.57 g/mol	
Temperature	293(2) K	
Wavelength	0.71073 Å	
Crystal system	Monoclinic	
Space group	$P2_1/n$	
Unit cell dimensions	a = 11.3680(8) Å b = 11.1648(8) Å c = 15.8593(11) Å	$\alpha = 90^\circ$ $\beta = 103.563(2)^\circ$ $\gamma = 90^\circ$
Volume	1956.8(2) Å ³	
Z	4	
Density (calculated)	1.940 g/cm ³	
Absorption coefficient	5.217 mm ⁻¹	
F(000)	1104	
Theta range for data collection	2.00 to 28.32°	
Index ranges	$-15 \leq h \leq 12, -14 \leq k \leq 14, -21 \leq l \leq 21$	
Reflections collected	35,784	
Independent reflections	4833 [R(int) = 0.0831]	
Completeness to theta = 28.50°	99.20%	
Refinement method	Full-matrix least-squares on F ²	
Data/restraints/parameters	4833/0/231	
Goodness-of-fit on F ²	1.162	
Final R indices [I > 2sigma(I)]	R1 = 0.0820, wR2 = 0.1488	
R indices (all data)	R1 = 0.1301, wR2 = 0.1643	
Largest diff. peak and hole	1.976 and -1.721	

Table 2. Selected bond distances (Å) and angles (°) for the $[Cd(BPMT)Br_2]$ complex.

Bond	Distance	Bond	Distance
Cd1-N4	2.337(6)	Cd1-Br1	2.5388(11)
Cd1-N1	2.413(7)	Cd1-Br2	2.5527(13)
Cd1-N11	2.417(7)		
Bond	Angle	Bond	Angle
N4-Cd1-N1	66.0(2)	N11-Cd1-Br1	103.27(17)
N4-Cd1-N11	66.0(2)	N4-Cd1-Br2	107.55(17)
N1-Cd1-N11	129.8(2)	N1-Cd1-Br2	104.37(19)
N4-Cd1-Br1	136.50(17)	N11-Cd1-Br2	103.25(18)
N1-Cd1-Br1	101.05(16)	Br1-Cd1-Br2	115.94(4)

The supramolecular structure of the $[Cd(BPMT)Br_2]$ complex is controlled by the intermolecular Br...H interactions shown in Figure 3A. These non-classical interactions are generally weak, and they occur between the coordinated bromide ion as a hydrogen-bond acceptor and the C-H bonds from the methyl and pyrazolyl moieties of BPMT ligand as a hydrogen-bond donor. The hydrogen-bond parameters and the packing scheme are depicted in Table 3 and Figure 3B. In the structurally related $[Cd(BPMT)Cl_2]$ complex, the packing is mainly controlled by Cl...H interactions where the donor-acceptor distance is 3.636(4) Å, which is shorter than the corresponding values for the dibromo complex (Table 3).

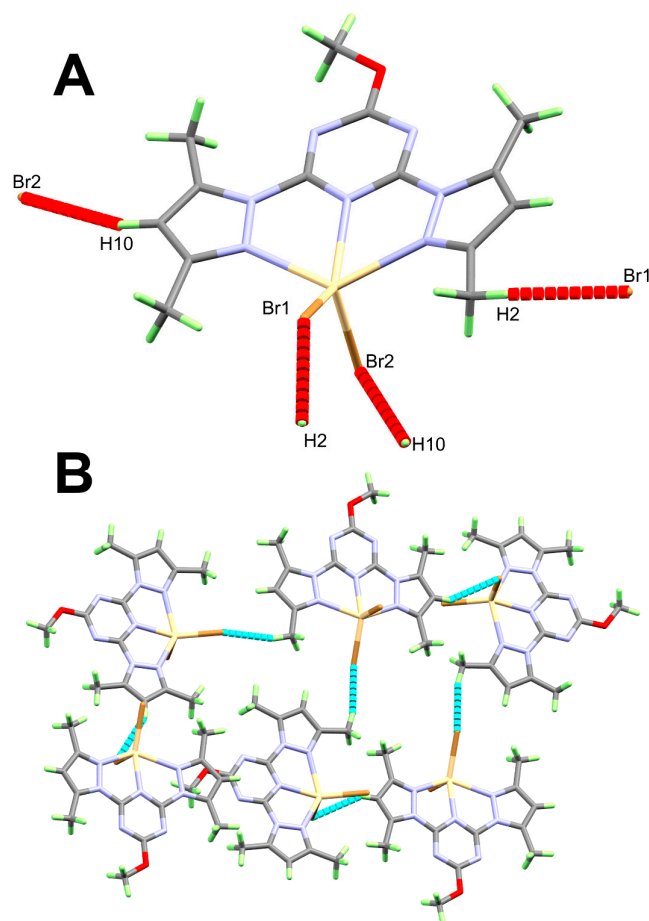


Figure 3. Important contacts (A) and packing scheme (B) in the $[\text{Cd}(\text{BPMT})\text{Br}_2]$ complex.

Table 3. Hydrogen-bond parameters in the $[\text{Cd}(\text{BPMT})\text{Br}_2]$ complex.

Atoms	D-H (Å)	H...A (Å)	D...A (Å)	D-H...A (°)	Symm. Code
C2-H2...Br1	0.96	2.91	3.830(10)	161	$1/2 - x, -1/2 + y, 1/2 - z$
C10-H10...Br2	0.93	3.004	3.835(8)	149.6	$-1/2 + x, 1.5 - y, -1/2 + z$

3.3. Hirshfeld Analysis

Hirshfeld analysis of molecular packing is performed in order to further analyze the different contacts in the crystal structure at both quantitative and qualitative levels. Different contacts were decomposed and their percentages were depicted in Figure 4.

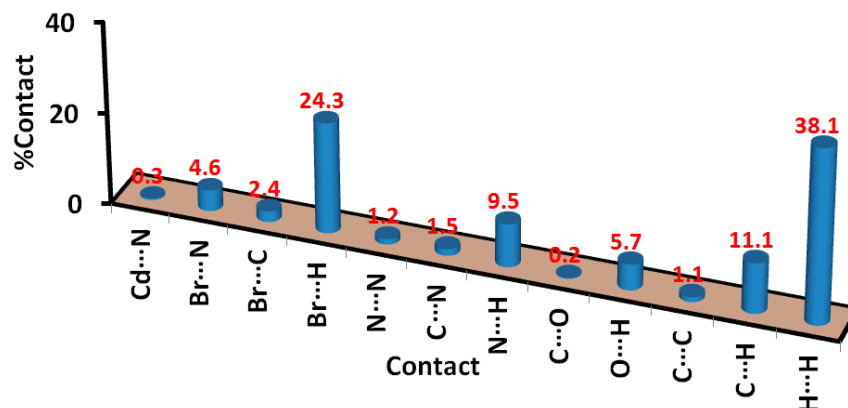


Figure 4. Percentages of all intermolecular contacts in the $[\text{Cd}(\text{BPMT})\text{Br}_2]$ complex.

It is clear that the H···H, Br···H, C···H, and N···H are the most dominant interactions in the crystal structure of the [Cd(BPMT)Br₂] complex; their percentages are 38.1, 24.3, 11.1, and 9.5% from the whole contacts that occurred in the crystal. Other contacts such as O···H (5.7%), Br···N (4.6%), and Br···C (2.4%) have low percentages. Analysis of the d_{norm} map indicated that the presence of red spots related only to the Br···H, C···H, and Br···C contacts (Figure 5). These red regions indicated contacts having shorter distances than the vdWs radii sum of the interacting atoms. Other contacts appeared as blue and white regions in the d_{norm} map. Hence, these interactions are considered less significant in the molecular packing since the corresponding interaction distances are longer or equal than the vdWs radii sum of the interacting atoms, respectively. The regions shared in the Br···H, Br···C, and C···H interactions are labeled as A–C, respectively in the d_{norm} map (Figure 5). In the structurally related [Cd(BPMT)Cl₂] complex, the percentages of the H···H, Cl···H, C···H, and N···H are 37.7, 24.5, 11.4, and 10.1%, respectively, whereas the O···H (6.1%), Cl···N (3.1%), and Cl···C (2.0%) contacts are less dominant. Additionally, the Cl···H, C···H, and Cl···C contacts are the most important in the molecular packing of this complex.

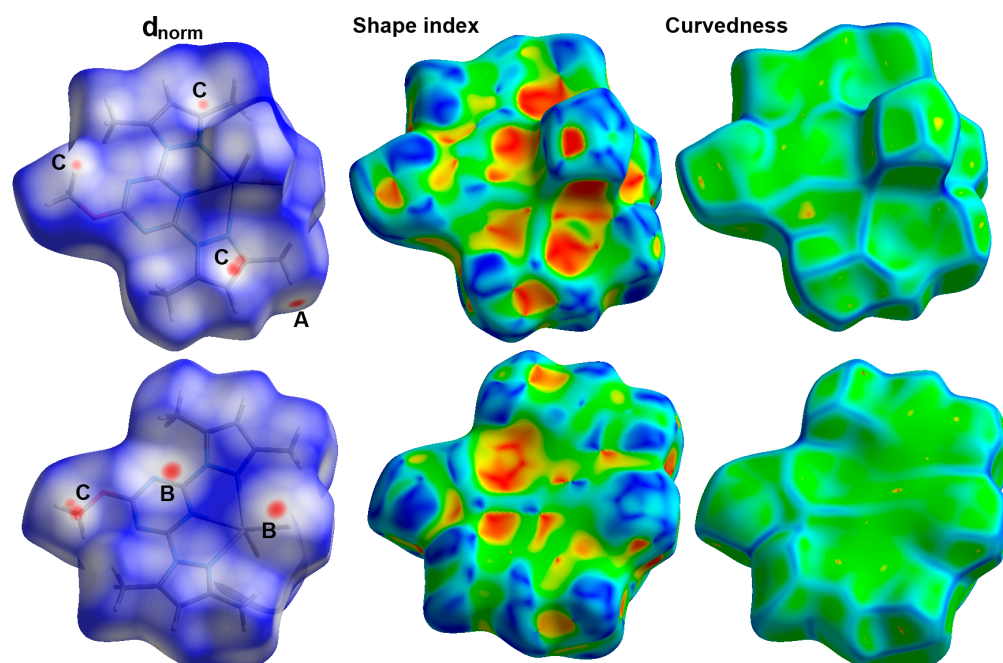


Figure 5. Hirshfeld surfaces of the [Cd(BPMT)Br₂] complex. The shape index and curvedness maps revealed the absence of aromatic π - π stacking interactions.

On the other hand, analysis of the fingerprint plots for the Br···H, C···H, and Br···C contacts further confirmed that these interactions occur at short interaction distances (Figure 6). The shortest Br···H contacts are Br2···H10 (2.873 Å) and Br1···H2 (2.792 Å) whereas the C1···H15 (2.718 Å), C3···H15 (2.683 Å), and C12···H16 (2.720 Å) are the shortest C-H··· π interactions. Interestingly, the short Br1···C7 (3.405 Å) between the coordinated bromide anion and the *s*-triazine core belong to the anion- π stacking interactions, which is considered as a general feature for metal complexes of the electron deficient *s*-triazine type ligands [47–50].

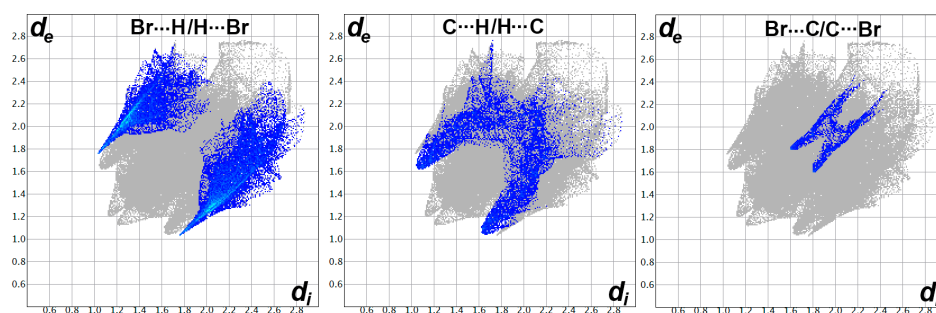


Figure 6. The decomposed fingerprint of the important interactions in the $[\text{Cd}(\text{BPMT})\text{Br}_2]$ complex.

3.4. Biological Studies

The $[\text{Cd}(\text{BPMT})\text{Br}_2]$ complex was tested for its antibacterial and antifungal activities. The results were compared with the free **BPMT**, as well as Gentamycin and Ketoconazole as antibacterial and antifungal controls, respectively (Table 4). The Cd(II) complex has a broad spectrum of antibacterial activity against both Gram-positive and Gram-negative bacterial strains with inhibition zones ranging from 18 mm (*E. coli*) to 44 mm (*B. subtilis*). In the case of *S. aureus* and *P. vulgaris*, the inhibition zone diameters are 23 and 25 mm, respectively. The free **BPMT** has no antibacterial activity against these microbes except *S. aureus* (8 mm). Hence, the Cd(II) complex is a better antibacterial agent than the free ligand. Additionally, the Cd(II) complex has better antibacterial activity against *B. subtilis* than Gentamycin (26 mm). The sizes of the inhibition zones are the same in the case of *P. vulgaris* and *C. albicans* (20 mm), which are similar to Gentamycin and Ketoconazole as controls. Hence, the Cd(II) complex has good antifungal activity against *C. albicans* whereas it is not active against *A. fumigatus* at the applied concentration. In addition, the results were compared with the $[\text{Zn}(\text{BPMT})(\text{NCS})_2]$ and $[\text{Zn}(\text{BPMT})(\text{Br})_2]$ analogs at the same experimental conditions [62]. The $[\text{Cd}(\text{BPMT})\text{Br}_2]$ complex has better antibacterial activity against the Gram-positive bacteria than any of the two Zn(II) complexes where the inhibition zone diameters are in the range of 16–33 mm. In contrast, the $[\text{Zn}(\text{BPMT})(\text{NCS})_2]$ complex has better antibacterial activity against the Gram-negative bacteria *E. coli* (20 mm) and *P. vulgaris* (26 mm) than the $[\text{Cd}(\text{BPMT})\text{Br}_2]$ complex. In terms of antifungal activity, all three complexes exhibited no activity against *A. fumigatus*. For *C. albicans*, the $[\text{Cd}(\text{BPMT})\text{Br}_2]$ complex has higher activity than the $[\text{Zn}(\text{BPMT})(\text{NCS})_2]$ complex (12 mm) whereas the $[\text{Zn}(\text{BPMT})(\text{Br})_2]$ showed no action against this microbe.

Table 4. Zone of inhibition (mm) for **BPMT** and the $[\text{Cd}(\text{BPMT})\text{Br}_2]$ complex.

Microbe	$[\text{Cd}(\text{BPMT})\text{Br}_2]$	BPMT	Control
<i>A. fumigatus</i>	NA	NA	17 ^a
<i>C. albicans</i>	20	NA	20 ^a
<i>S. aureus</i>	23	8	24 ^b
<i>B. subtilis</i>	44	NA	26 ^b
<i>E. coli</i>	18	NA	30 ^b
<i>P. vulgaris</i>	25	NA	25 ^b

^a Ketoconazole, ^b Gentamycin.

In addition, the anticancer activity of the $[\text{Cd}(\text{BPMT})\text{Br}_2]$ complex against lung cancer cells (A-549) was evaluated (Figure 7). The IC_{50} value of the $[\text{Cd}(\text{BPMT})\text{Br}_2]$ complex was found to be $18.64 \pm 1.09 \mu\text{g}/\text{mL}$, whereas for **BPMT** and *cis*-platin, the IC_{50} values are 372.79 ± 13.64 and $7.53 \pm 0.69 \mu\text{g}/\text{mL}$, respectively. It is clear that the Cd(II) complex has better anticancer activity than free **BPMT** ligand although its anticancer activity is close to the well-known anticancer agent *cis*-platin. Additionally, the cytotoxic activity of the $[\text{Cd}(\text{BPMT})\text{Br}_2]$ complex is compared with the $[\text{Zn}(\text{BPMT})(\text{NCS})_2]$ and $[\text{Zn}(\text{BPMT})(\text{Br})_2]$ complexes [62]. At the same experimental conditions, the IC_{50} values for the Zn(II) complexes are determined to be 43.86 ± 3.12 and $30.23 \pm 1.26 \mu\text{g}/\text{mL}$, respectively. It is obvious

that the studied Cd(II) complex has better cytotoxic activity than the two Zn(II) complexes against lung cancer cells (A-549).

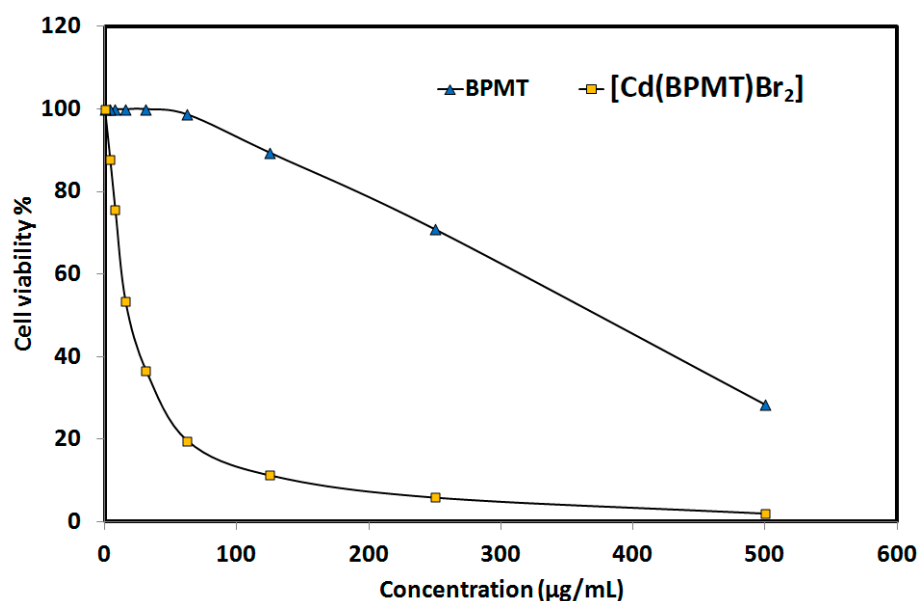


Figure 7. Cytotoxic activity of the $[Cd(BPMT)Br_2]$ complex against lung cancer cells (A-549). The detailed results are tabulated in Tables S1 and S2.

4. Conclusions

The synthesis, characterization, and X-ray structure of the new $[Cd(BPMT)Br_2]$ complex were reported. The Cd(II) is penta-coordinated with one tridentate **BPMT** ligand and two bromide groups. The CdN_3Br_2 coordination sphere has a slightly distorted square pyramidal configuration. The packing is controlled by many short intermolecular contacts such as the $Br \cdots H$, $C \cdots H$, and $Br \cdots C$ interactions as revealed from the Hirshfeld analysis. The Cd(II) complex showed interesting antibacterial activity against Gram-positive and Gram-negative bacteria. Its antibacterial potency outperformed Gentamycin against *B. subtilis*. Additionally, it has similar activity against *P. vulgaris* and *C. albicans* compared to Gentamycin and Ketoconazole as antibacterial and antifungal controls, respectively. In addition, the Cd(II) complex has higher cytotoxicity towards lung cancer cells (A-549) than the free **BPMT** ligand.

Supplementary Materials: The following supporting information can be downloaded at: <https://www.mdpi.com/article/10.3390/cryst12060861/s1>, Figure S1: FTIR spectra of the $[Cd(BPMT)Br_2]$ complex; Figure S2: FTIR spectra of **BPMT**; Method S1: Synthesis of **BPMT**; Scheme S1: Synthesis of the ligand (**BPMT**); Method S2: Antimicrobial studies; Method S3: Evaluation of Cytotoxic activity; Table S1: Evaluation of cytotoxicity of $[Cd(BPMT)Br_2]$ against A-549 cell line; Table S2: Evaluation of cytotoxicity of **BPMT** against A-549 cell line. Chemicals and instrumentations; X-ray structure measurement details. References [51–60] are cited in the supplementary materials.

Author Contributions: Conceptualization, H.M.R., A.E.-F. and S.M.S.; methodology, H.M.R. and S.M.S.; software, S.M.S. and N.D.; formal analysis, K.A.D., H.M.R., A.A.M.A., N.D., A.E.-F. and S.M.S.; investigation, A.A.M.A. and H.M.R.; resources, K.A.D., H.M.R., A.E.-F., N.D., A.A.M.A. and S.M.S.; writing—original draft preparation, K.A.D., H.M.R., A.E.-F., N.D., A.A.M.A. and S.M.S.; writing—review and editing, H.M.R., A.E.-F., N.D. and S.M.S.; supervision, H.M.R., A.E.-F. and S.M.S. All authors have read and agreed to the published version of the manuscript.

Funding: This project was funded by the Researchers Supporting Project number (RSP-2021/388), King Saud University, Riyadh, Saudi Arabia.

Institutional Review Board Statement: Not applicable.

Informed Consent Statement: Not applicable.

Data Availability Statement: Not applicable.

Acknowledgments: The authors extend their sincere appreciation to the Researchers Supporting Project number (RSP-2021/388), King Saud University, Riyadh, Saudi Arabia.

Conflicts of Interest: The authors declare no conflict of interest.

References

1. Raja, D.S.; Bhuvanesh, N.S.P.; Natarajan, K. Synthesis, crystal structure and pharmacological evaluation of two new Cu(II) complexes of 2-oxo-1,2-dihydroquinoline-3-carbaldehyde (benzoyl)hydrazine: A comparative investigation. *Eur. J. Med. Chem.* **2012**, *47*, 73–85. [[CrossRef](#)] [[PubMed](#)]
2. Ignatius, I.C.; Rajathi, S.; Kirubavathi, K.; Selvaraju, K. Synthesis, crystal growth and characterization of novel semiorganic nonlinear optical crystal: Dichloro(beta-alanine)cadmium(II). *Optik* **2014**, *125*, 5144–5147. [[CrossRef](#)]
3. Saghatforoush, L.; Khoshtarkib, Z.; Keypour, H.; Hakimi, M. Mononuclear, tetranuclear and polymeric cadmium(II) complexes with the 3,6-bis(2-pyridyl)-1,2,4,5-tetrazine ligand: Synthesis, crystal structure, spectroscopic and DFT studies. *Polyhedron* **2016**, *119*, 160–174. [[CrossRef](#)]
4. Wang, W.; Qiao, J.; Wang, L.; Duan, L.; Zhang, D.; Yang, W.; Qiu, Y. Synthesis, structures, and optical properties of cadmium iodide/phenethylamine hybrid materials with controlled structures and emissions. *Inorg. Chem.* **2007**, *46*, 10252–10260. [[CrossRef](#)] [[PubMed](#)]
5. Mlowe, S.; Lewis, D.J.; Malik, M.A.; Raftery, J.; Mubofu, E.B.; O'Brien, P.; Revaprasadu, N. Bis(piperidinedithiocarbamate)-pyridinecadmium(ii) as a single-source precursor for the synthesis of CdS nanoparticles and aerosol-assisted chemical vapour deposition (AACVD) of CdS thin films. *New J. Chem.* **2014**, *38*, 6073–6080. [[CrossRef](#)]
6. Hashemi, L.; Hosseinifard, M.; Amani, V.; Morsali, A.J. Sonochemical Synthesis of Two New Nano-structured Cadmium(II) Supramolecular Complexes. *Inorg. Organomet. Polym.* **2013**, *23*, 519–524. [[CrossRef](#)]
7. Biswas, F.B.; Roy, T.G.; Rahman, A.; Emran, T.B. An in vitro antibacterial and antifungal effects of cadmium(II) complexes of hexamethyltetraazacyclotetradecadiene and isomers of its saturated analogue. *Asian. Pac. J. Trop. Med.* **2014**, *7*, S534–S539. [[CrossRef](#)]
8. Yi, X.C.; Huang, M.X.; Qi, Y.; Gao, E.Q. Synthesis, structure, luminescence and catalytic properties of cadmium(ii) coordination polymers with 9H-carbazole-2,7-dicarboxylic acid. *Dalton Trans.* **2014**, *43*, 3691–3697. [[CrossRef](#)]
9. Jia, W.G.; Li, D.D.; Gu, C.; Dai, Y.C.; Zhou, Y.H.; Yuan, G.; Sheng, E.H. Two cadmium(II) complexes with oxazoline-based ligands as effective catalysts for C–N cross-coupling reactions. *Inorg. Chim. Acta* **2015**, *427*, 226–231. [[CrossRef](#)]
10. Zhang, F.; Zheng, X.-L.; Lin, Q.-Y.; Wang, P.-P.; Song, W.-J. Two novel cadmium(II) complexes with demethylcantharate and polypyridyl: Crystal structure, interactions with DNA and bovine serum albumin. *Inorg. Chim. Acta* **2013**, *394*, 85–91. [[CrossRef](#)]
11. Bjelogrić, S.; Todorović, T.; Bacchi, A.; Zec, M.; Sladić, D.; Srdić-Rajić, T.; Radanović, D.; Radulović, S.; Pelizzi, G.; Anđelković, K. Synthesis, structure and characterization of novel Cd(II) and Zn(II) complexes with the condensation product of 2-formylpyridine and selenosemicarbazide Antiproliferative activity of the synthesized complexes and related selenosemicarbazone complexes. *J. Inorg. Biochem.* **2010**, *104*, 673–682. [[CrossRef](#)] [[PubMed](#)]
12. Alomar, K.; Landreau, A.; Kempf, M.; Khan, M.A.; Allain, M.; Bouet, G. Synthesis, crystal structure, characterization of zinc(II), cadmium(II) complexes with 3-thiophene aldehyde thiosemicarbazone (3TTSCH). Biological activities of 3TTSCH and its complexes. *J. Inorg. Biochem.* **2010**, *104*, 397–404. [[CrossRef](#)] [[PubMed](#)]
13. Tai, Y.-X.; Ji, Y.-M.; Lu, Y.-L.; Li, M.-X.; Wu, Y.-Y.; Han, Q.-X. Cadmium(II) and indium(III) complexes derived from 2-benzoylpyridine *N*(4)-cyclohexylthiosemicarbazone: Synthesis, crystal structures, spectroscopic characterization and cytotoxicity. *Synth. Met.* **2016**, *219*, 109–114. [[CrossRef](#)]
14. Hossain, Z.; Huq, F. Studies on the interaction between Cd²⁺ ions and DNA. *J. Inorg. Biochem.* **2002**, *90*, 85–96. [[CrossRef](#)]
15. Filipović, N.R.; Bacchi, A.; Lazić, M.; Pelizzi, G.; Radulović, S.; Sladić, D.M.; Todorović, T.R.; Anđelković, K.K. Structure and Cytotoxic Activity Evaluation of a Dinuclear Complex of Cd(II) with *N*, *N*'-bis[(1E)-1-(2-pyridyl)ethylidene]propanedihydrazide. *Inorg. Chem. Commun.* **2008**, *11*, 47–50. [[CrossRef](#)]
16. Soliman, S.M.; El-Faham, A. Synthesis and structure diversity of high coordination number Cd(II) complexes of large *s*-triazine bis-Schiff base pincer chelate. *Inorg. Chim. Acta* **2019**, *488*, 131–140. [[CrossRef](#)]
17. Mandal, S.; Saha, R.; Saha, M.; Pradhan, R.; Butcher, R.J.; Saha, N.C. Synthesis, crystal structure, spectral characterization and photoluminescence property of three Cd(II) complexes with a pyrazole based Schiff-base ligand. *J. Mol. Struct.* **2016**, *1110*, 11–18. [[CrossRef](#)]
18. Ali, M.A.; Mirza, A.H.; Nazimuddin, M.; Rahman, H.; Butcher, R.J. The preparation and characterization of mono- and bis-chelated cadmium(II) complexes of the di-2-pyridylketone Schiff base of *S*-methylthiocarbamate (Hdpsme) and the X-ray crystal structure of the [Cd(dpksme)₂].0.5MeOH complex. *Trans. Met. Chem.* **2002**, *27*, 268–273.
19. Mua, Y.; Xie, J.; Ran, Y.; Han, B.; Qin, G. A series of entangled Cd(II) coordination polymers assembled from different dicarboxylate acids and a flexible imidazole-based ligand. *Polyhedron* **2015**, *89*, 20–28. [[CrossRef](#)]
20. Majumder, A.; Rosair, G.M.; Mallick, A.; Chattopadhyay, N.; Mitra, S. Synthesis, structures and fluorescence of nickel, zinc and cadmium complexes with the *N,N,O*-tridentate Schiff base *N*-2-pyridylmethylidene-2-hydroxy-phenylamine. *Polyhedron* **2006**, *25*, 1753–1762. [[CrossRef](#)]

21. Lowther, M.D.; Wacholtz, W.F.; Mague, J.T. A luminescent heteroleptic five-coordinate cadmium(II) complex containing a bridging dithiolate ligand. *J. Chem. Cryst.* **2001**, *31*, 295–300. [[CrossRef](#)]
22. Ray, S.; Konar, S.; Jana, A.; Jana, S.; Patra, A.; Chatterjee, S.; Golen, J.A.; Rheingold, A.L.; Mandal, S.S.; Kar, S.K. Three new pseudohalide bridged dinuclear Zn(II), Cd(II) complexes of pyrimidine derived Schiff base ligands: Synthesis, crystal structures and fluorescence studies. *Polyhedron* **2012**, *33*, 82–89. [[CrossRef](#)]
23. Abu-Youssef, M.A.M.; Langer, V. 1D, 2D and 3D cadmium(II) polymeric complexes with quinoline-4-carboxylate anion, quinazoline and 2,5-dimethylpyrazine. *Polyhedron* **2006**, *25*, 1187–1194. [[CrossRef](#)]
24. Vickers, S.M.; Frischmann, P.D.; MacLachlan, M.J. Family of Cadmium Acetate Coordination Networks With Structurally Diverse $[\text{Cd}_4(\text{OAc})_9(\mu^3\text{-OH})]^{2-}$ Secondary Building Units. *Inorg. Chem.* **2011**, *50*, 2957–2965. [[CrossRef](#)] [[PubMed](#)]
25. Moulton, C.J.; Shaw, B.L. Transition metal–carbon bonds. Part XLII. Complexes of nickel, palladium, platinum, rhodium and iridium with the tridentate ligand 2,6-bis[(di-*t*-butylphosphino)methyl]phenyl. *J. Chem. Soc. Dalton Trans.* **1976**, 1020–1040. [[CrossRef](#)]
26. Van Koten, G. Tuning the reactivity of metals held in a rigid ligand environment. *Pure Appl. Chem.* **1989**, *61*, 1681–1694. [[CrossRef](#)]
27. Albrecht, M.; Van Koten, G. Platinum Group Organometallics Based on “Pincer” Complexes: Sensors, Switches, and Catalysts. *Angew. Chem. Int. Ed. Engl.* **2001**, *40*, 3750–3781. [[CrossRef](#)]
28. Asay, M.; Morales-Morales, D. Non-symmetric pincer ligands: Complexes and applications in catalysis. *J. Chem. Soc. Dalton Trans.* **2015**, *44*, 17432–17447. [[CrossRef](#)]
29. Li, H.; Zheng, B.; Huang, K.-W. A new class of PN_3 -pincer ligands for metal–ligand cooperative catalysis. *Coord. Chem. Rev.* **2015**, *293*, 116–138. [[CrossRef](#)]
30. Szabó, K.J. Mechanism of the oxidative addition of hypervalent iodonium salts to palladium(II) pincer-complexes. *J. Mol. Catal. A Chem.* **2010**, *324*, 56–63. [[CrossRef](#)]
31. De Hoog, P.; Gamez, P.; Driessen, L.W.; Reedijk, J. New polydentate and polynucleating *N*-donor ligands from amines and 2,4,6-trichloro-1,3,5-triazine. *Tetrahedron Lett.* **2002**, *43*, 6783–6786. [[CrossRef](#)]
32. Das, A.; Demeshko, S.; Dechert, S.; Meyer, F. A New Triazine-Based Tricompartamental Ligand for Stepwise Assembly of Mononuclear, Dinuclear, and 1D-Polymeric Heptacoordinate Manganese(II)/Azido Complexes. *Eur. J. Inorg. Chem.* **2011**, *2011*, 1240–1248. [[CrossRef](#)]
33. Medlycott, E.A.; Udachin, K.A.; Hanan, G.S. Non-covalent polymerisation in the solid state: Halogen–halogen *vs.* methyl–methyl interactions in the complexes of 2,4-di(2-pyridyl)-1,3,5-triazine ligands. *Dalton Trans.* **2007**, 430–438. [[CrossRef](#)]
34. Mooibroek, T.J.; Gamez, P. The *s*-triazine ring, a remarkable unit to generate supramolecular interactions. *Inorg. Chim. Acta* **2007**, *360*, 381–404. [[CrossRef](#)]
35. Gamez, P.; Reedijk, J. 1,3,5-Triazine-Based Synthons in Supramolecular Chemistry. *Eur. J. Inorg. Chem.* **2006**, *2006*, 29–42. [[CrossRef](#)]
36. Ranganathan, A.; Heisen, B.C.; Dix, I.; Meyer, F. A triazine-based three-directional rigid-rod tecton forms a novel 1D channel structure. *Chem. Commun.* **2007**, 3637–3639. [[CrossRef](#)] [[PubMed](#)]
37. Galan-Mascaros, J.R.; Clemente-Juan, J.M.; Dunbar, K.R. Synthesis, structure and magnetic properties of the one-dimensional chain compound $[\text{K}[\text{Fe}(\text{1,3,5-triazine-2,4,6-tricarboxylate})(\text{H}_2\text{O})_2] \cdot 2\text{H}_2\text{O}]_\infty$. *J. Chem. Soc. Dalton Trans.* **2002**, 2710–2713. [[CrossRef](#)]
38. Wietzke, R.; Mazzanti, M.; Latour, J.M.; Percaut, J. Crystal Structure and Solution Fluxionality of Lanthanide Complexes of 2,4,6-Tris(2-pyridyl)-1,3,5-triazine. *Inorg. Chem.* **1999**, *38*, 3581–3585. [[CrossRef](#)]
39. Ramirez, J.; Stadler, A.-M.; Kyritskas, N.; Lehn, J.-M. Solvent-modulated reversible conversion of a $[2 \times 2]$ -grid into a pincer-like complex. *Chem. Commun.* **2007**, 237–239. [[CrossRef](#)]
40. Ramirez, J.; Stadler, A.M.; Harrowfield, J.M.; Brelot, L.; Huuskonen, J.; Rissanen, K.; Allouche, L.; Lehn, J.M. Coordination Architectures of Large Heavy Metal Cations (Hg^{2+} and Pb^{2+}) with Bis-tridentate Ligands: Solution and Solid-State Studies. *Z. Anorg. Allg. Chem.* **2007**, *633*, 2435–2444. [[CrossRef](#)]
41. Ramirez, J.; Stadler, A.-M.; Brelot, L.; Lehn, J.-M. Coordinative, conformational and motional behaviour of triazine-based ligand strands on binding of Pb(II) cations. *Tetrahedron* **2008**, *64*, 8402–8410. [[CrossRef](#)]
42. Hsu, G.-Y.; Misra, P.; Cheng, S.-C.; Wei, H.-H.; Mohanta, S. Syntheses, structures, and magnetic properties of dicyanamide bridged one-dimensional double chain and discrete dinuclear complexes of manganese(II) derived from 6,7-dimethyl-2,3-di(2-pyridyl)quinoxaline or 2,4,6-tri(2-pyridyl)-1,3,5-triazine. *Polyhedron* **2006**, *25*, 3393–3398. [[CrossRef](#)]
43. Zhang, M.; Fang, R.; Zhao, Q. Synthesis and Crystal Structure of $[\text{Mn}(\text{H}_2\text{O})(\text{tptz})(\text{CH}_3\text{COO})][\text{N}(\text{CN})_2] \cdot 2\text{H}_2\text{O}$ ($\text{tptz} = 2,4,6\text{-tris}(2\text{-pyridyl})\text{-1,3,5-triazine}$). *J. Chem. Crystallogr.* **2008**, *38*, 601–604. [[CrossRef](#)]
44. Tyagi, P.; Singh, U.P. Chloro and azido bonded manganese complexes: Synthesis, structural, and magnetic studies. *J. Coord. Chem.* **2009**, *62*, 1613–1622. [[CrossRef](#)]
45. Soliman, S.M.; El-Faham, A. One pot synthesis of two Mn(II) perchlorate complexes with *s*-triazine *NNN*-pincer ligand; molecular structure, Hirshfeld analysis and DFT studies. *J. Mol. Struct.* **2018**, *1164*, 344–353. [[CrossRef](#)]
46. Soliman, S.M.; El-Faham, A. Synthesis, Molecular and Supramolecular Structures of New Mn(II) Pincer-Type Complexes with *s*-Triazine Core Ligand. *J. Coord. Chem.* **2018**, *71*, 2373–2388. [[CrossRef](#)]
47. Soliman, S.M.; Elsilik, S.E.; El-Faham, A. Syntheses, structure, Hirshfeld analysis and antimicrobial activity of four new Co(II) complexes with *s*-triazine-based pincer ligand. *Inorg. Chim. Acta* **2020**, *510*, 119753. [[CrossRef](#)]

48. Soliman, S.M.; El-Faham, A. Synthesis, molecular structure and DFT studies of two heteroleptic nickel(II) s-triazine pincer type complexes. *J. Mol. Struct.* **2019**, *1185*, 461–468. [CrossRef]
49. Soliman, S.M.; Elsilk, S.E.; El-Faham, A. Synthesis, structure and biological activity of zinc(II) pincer complexes with 2,4-bis(3,5-dimethyl-1H-pyrazol-1-yl)-6-methoxy-1,3,5-triazine. *Inorg. Chim. Acta* **2020**, *508*, 119627. [CrossRef]
50. Soliman, S.M.; El-Faham, A. Synthesis, X-ray structure, and DFT studies of five- and eight-coordinated Cd(II) complexes with s-triazine N-pincer chelate. *J. Coord. Chem.* **2019**, *73*, 1621–1636. [CrossRef]
51. Barakat, A.; El-Faham, A.; Haukka, M.; Al-Majid, A.M.; Soliman, S.M. s-Triazine Pincer Ligands: Synthesis of their Metal Complexes, Coordination Behavior, and Applications. *App. Organomet. Chem.* **2021**, *35*, e6317. [CrossRef]
52. Sheldrick, G.M. SHELXT—Integrated space-group and crystal-structure determination. *Acta Cryst. A* **2015**, *71*, 3–8. [CrossRef] [PubMed]
53. Sheldrick, G.M. Crystal structure refinement with SHELXL. *Acta Cryst. C* **2015**, *71*, 3–8. [CrossRef]
54. Farrugia, L.J. WinGX and ORTEP for Windows: An update. *J. Appl. Crystallogr* **2012**, *45*, 849–854. [CrossRef]
55. Bruker. APEX2, SAINT, SADABS, and XSELL; Bruker AXS Inc.: Madison, WI, USA, 2013.
56. Macrae, C.F.; Sovago, I.; Cottrell, S.J.; Galek, P.T.A.; McCabe, P.; Pidcock, E.; Platings, M.; Shields, G.P.; Stevens, J.S.; Towler, M.; et al. Mercury 4.0: From visualization to analysis, design and prediction. *J. Appl. Cryst.* **2020**, *53*, 226–235. [CrossRef]
57. Sheldrick, G.M. SADABS-2012/1. Bruker/Siemens Area Detector Absorption Correction Program; Bruker AXS Inc.: Madison, WI, USA, 2012.
58. Turner, M.J.; McKinnon, J.J.; Wolff, S.K.; Grimwood, D.J.; Spackman, P.R.; Jayatilaka, D.; Spackman, M.A. Crystal Explorer 17 University of Western Australia. 2017. Available online: <http://hirshfeldsurface.net> (accessed on 25 May 2018).
59. Clinical and Laboratory Standards Institute (CLSI). *Twentieth Informational Supplement*; M100-S22; Clinical and Laboratory Standards Institute: Wayne, PA, USA, 2012.
60. Mosmann, T. Rapid colorimetric assay for cellular growth and survival: Application to proliferation and cytotoxicity assays. *J. Immunol. Methods* **1983**, *65*, 55–63. [CrossRef]
61. Addison, A.W.; Rao, T.N.; Reedijk, J.; Rijn, J.V.; Verschoor, G.C. Synthesis, structure, and spectroscopic properties of copper(II) compounds containing nitrogen–sulphur donor ligands; the crystal and molecular structure of aqua [1,7-bis(*N*-methylbenzimidazol-2'-yl)-2,6-dithiaheptane]copper(II) perchlorate. *J. Chem. Soc. Dalton Trans.* **1984**, 1349–1356. [CrossRef]
62. Refaat, H.M.; Alotaibi, A.A.M.; Dege, N.; El-Faham, A.; Soliman, S.M. Synthesis, Structure and Biological Evaluations of Zn(II) Pincer Complexes Based on S-Triazine Type Chelator. *Molecules* **2022**, *27*, 3625. [CrossRef] [PubMed]